PHYSICAL REVIEW D VOLUME 15, NUMBER 3 1 FEBRUARY 1977

Helicity conservation and meson diffraction dissociation*

Edmond L. Berger
High Energy Physics Division, Argonne National Laboratory, Argonne, Illinois 60439

J. T. Donohue
High Energy Physics Division, Argonne National Laboratory, Argonne, Illinois 60439
and Laboratoire de Physique Théorique,†‡ Université de Bordeaux I Gradignan, France
(Received 4 October 1976)

In a Deck-model description of meson diffraction dissociation, we study the contribution made to the low-mass enhancement by the vector-meson-exchange Deck amplitudes. The vector-exchange amplitudes are parametrized with the help of data on the electroproduction of ρ mesons. Cross sections for vector exchange are compared to the standard pseudoscalar-meson-exchange Deck results and are found to be comparable in specific cases. A detailed spin and helicity amplitude analysis shows that the vector-exchange Deck amplitudes provide a low-mass system which satisfies approximate s-channel helicity conservation, whereas the pseudoscalar-exchange terms yield approximate t-channel helicity conservation. Combining the two contributions, we show that approximate s-channel helicity conservation holds in $Kp \to (\rho K)p$ and in $Kp \to (\omega K)p$. However, t-channel helicity conservation is expected in $Kp \to (K^*\pi)p$, $\pi p \to (\rho\pi)p$, and $Kp \to (\phi K)p$. These results agree with data. The relevance of these results to the interpretation of the Q-meson-resonance region is discussed.

I. INTRODUCTION

Detailed experimental analyses have recently provided a wealth of information on the spins, parities, and helicity properties of hadronic states produced by diffractive dissociation.[1-5] In meson-dissociation reactions of the type $0^-p \to (1^-0^-)p$, it is observed that the low-mass vector-pseudoscalar system (1^-0^-) is formed predominantly as an S-wave $J^P = 1^+$ state. In two processes, $Kp \to (\rho K)p$ and $Kp \to (\omega K)p$, the helicity of the produced S-wave system is primarily zero when measured with respect to the *s-channel coordinate axes*.[2-4] By contrast, for $Kp \to (K^*\pi)p$ and $\pi p \to (\rho\pi)p$, the helicity is approximately zero with respect to the *t-channel axes*.[1,2,5] Less precise data on $\pi p \to (K^*\bar{K})p$ and on $Kp \to (\phi K)p$ suggest that t-channel helicity conservation also holds in these two cases.[1]

The Drell-Deck model has been invoked in attempts to explain many features of diffraction dissociation.[6] It has been known for some time that the model leads naturally to dominance of $J^P = 1^+$. In situations in which the pseudoscalar-exchange Deck graph dominates, the model also predicts approximate t-channel helicity conservation[7] for the $J^P = 1^+$ state. Until now, however, it was unclear whether the model could accommodate s-channel helicity conservation. In this article we perform a detailed helicity analysis of the model, including both pseudoscalar- and vector-exchange graphs. We conclude that the model leads to approximate s-channel helicity conservation for $Kp \to (\rho K)p$ and for $Kp \to (\omega K)p$, while it maintains approximate t-channel helicity conservation for $Kp \to (K^*\pi)p$, for $\pi p \to (\rho\pi)p$, and for $Kp \to (\phi K)p$. These results are in excellent accord with data.

The diagrams sketched in Fig. 1 show the pseudoscalar- and vector-exchange Deck graphs which generate low-mass diffractive enhancements. The vector-exchange contributions have often been neglected in the past for reasons not properly justified. Data are now known to require their inclusion. For example, the model with only π exchange predicts a crossover in the momentum-transfer distributions for $K^0p \to Q^0p$ and $\bar{K}^0p \to \bar{Q}^0p$ $(Q \to K^*\pi)$ in disagreement with data.[8] Inclusion of the K^* exchange was conjectured to remedy the error[9] and this is verified experimentally.[10] Appropriate selections on the decay angles in the Q rest frame allow separation of the two exchange contributions.[9,11] Motivated by this qualitative agreement with the crossover data and by the failure of the pseudoscalar term alone to provide s-channel helicity conservation where required, we examine the vector-exchange terms in detail. To our knowledge, the spin and helicity properties of these vector-exchange terms have not been addressed previously.

Our approach may first be sketched qualitatively for the prototype reaction $Kp \to (\rho K)p$. To specify the helicity properties of the vector-exchange graphs, we appeal to measurements[12] of the ρ helicity in the electroproduction process $ep \to ep\rho$, sketched in Fig. 2(a). From these data we deduce that transverse exchanged ρ's become ρ's of s-channel helicity ± 1 in the final state, whereas scalar exchanged ρ's are transformed into s-chan-

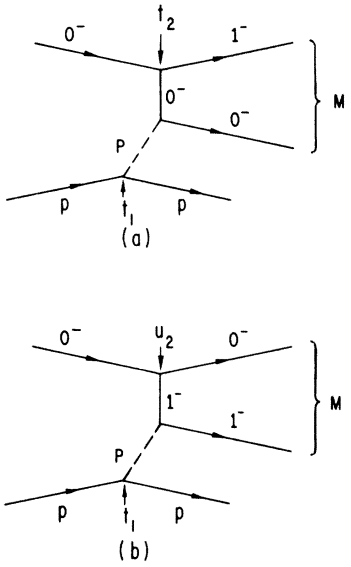

FIG. 1. Deck diagrams for the diffractive dissociation of a pseudoscalar-meson 0^- beam into a system of mass M composed of a vector 1^- and a pseudoscalar 0^- meson. Symbol P denotes the Pomeron. In (a), a pseudoscalar meson is exchanged, whereas in (b) a vector meson is exchanged.

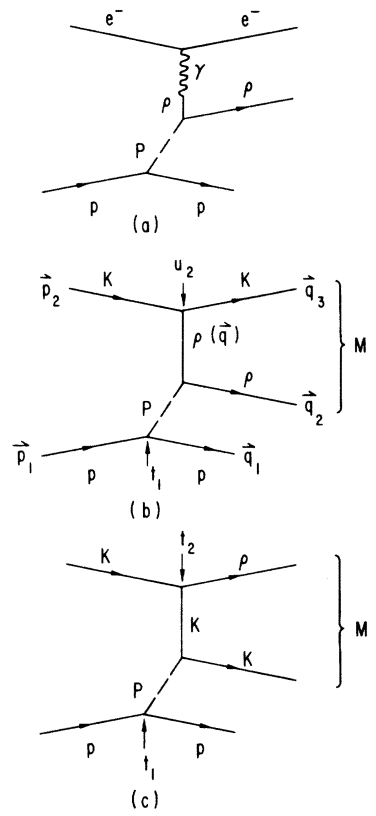

FIG. 2. (a) Vector-dominance diagram for the electroproduction process $ep \to e\rho p$. (b) ρ-exchange Deck diagram for $Kp \to (\rho K)p$. (c) Kaon-exchange Deck diagram for $Kp \to (\rho K)p$.

nel helicity-0 ρ mesons. Incorporating these measured properties of off-shell to on-shell ρp elastic scattering into the Deck amplitude, we derive the helicity properties of the ρ-exchange Deck graphs. In the model, the proportion of helicity-0 and helicity-1 ρ's is determined by the $\rho K\overline{K}$ coupling and the subsequent ρp scattering. Our conclusion is that the ρ-exchange Deck amplitude provides a final (ρK) S-wave system which is dominantly in the s-channel helicity-0 state. We then demonstrate numerically that the ρ-exchange graph yields a cross section which is comparable to that of the t-channel-helicity-conserving pseudoscalar K-exchange graph. We perform a partial-wave analysis of both the K- and ρ-exchange amplitudes. After combining the two contributions, our final result is a derivation of approximate s-channel helicity conservation in $Kp \to (\rho K)p$, in accord with data. For $\pi p \to (\rho\pi)p$ also, the ρ-exchange Deck graph yields a $(\rho\pi)$ system for which the s-channel helicity is predominantly zero. However, in this case, the t-channel-helicity-conserving π-exchange graph is dominant. The final result in $\pi p \to (\rho\pi)p$ is therefore an expectation of approximate t-channel helicity conservation.

We organize this article as follows. In Sec. II, we summarize the experimental situation, indicating more precisely what we understand by s- and t-channel helicity conservation. In Sec. III, we provide explicit pseudoscalar- and vector-exchange Deck *amplitudes* for $0^-p \to (1^-0^-)p$. A "direct" graph may also be considered in which the incident 0^- first scatters diffractively and then dissociates into a 1^-0^- system. Although potentially important, this diagram leads uniquely to a $J^P = 0^-$ final state. Because our concern here is the dominant $J^P = 1^+$ S-wave (1^-0^-) system, we ignore this third diagram. For the case of vector exchange, we discuss the various ingredients of the amplitudes in detail, showing how the electroproduction data are used to obtain amplitudes A_0 and A_1 for production of vector mesons with s-channel helicity 0 and 1, respectively. Cross sections are then computed, and we show the variation with momentum transfer of the two helicity contributions. We report a partial-wave analysis of the model, separating the S- and P-wave states in the final (1^-0^-) system for both the vector- and pseudoscalar-exchange amplitudes. We treat in turn the following processes: $Kp \to (\rho K)p$, $\pi p \to (\rho\pi)p$, $Kp \to (K^*\pi)p$, $Kp \to (\omega K)p$, $Kp \to (\phi K)p$, and $\pi p \to (K^*\overline{K})p$. Our conclusions are stated in Sec. IV.

II. APPROXIMATE HELICITY CONSERVATION

Data on the diffractive production of low-mass meson systems have been used to support various hypotheses such as t- or s-channel helicity conservation. As our partial-wave analyses show, the Deck model does not provide either exact s- or exact t-channel helicity conservation. Before discussing the detailed results of our investigation, we wish to summarize the experimental situation and to clarify some simple aspects of the problem.

Suppose the target and recoil nucleons are spinless, and that for a given produced state of quantum numbers J, l, the various (partial-wave) amplitudes $A_M^{J,l}(s, t_1, M^2)$ are in phase for different values of helicity M, as diffractive production might suggest. Then for the $J^P = 1^+$ state [e.g. the Q system in $Kp \to (K^*\pi)p$ or $Kp \to (\rho K)p$], the normalized spin density matrix can be diagonalized by a rotation about the normal to the scattering plane, yielding a matrix with $\rho_{00} = 1$. That is, there would be some direction in the Q rest frame, along which the Q would have spin projection zero ($M = 0$). The direction would be somewhere in the production plane. This implies that the density-matrix combination $\rho_{11} + \rho_{1-1}$ vanishes, as is observed.[5]

If the equal-phase and spinless-nucleon conditions were exact, there would *always* be some ideal choice of axis such that the spin projection is zero. This is illustrated in Fig. 3. We suppose that t_1' is such that the s- and t-channel quantization axes z_s and z_t, respectively, are oriented as shown. (At $t_1' = 0$, they are identical directions.) The double arrow shows four possible orientations out of an infinite number of our supposed ideal axis. Remembering that "approximate conservation" commonly means $\rho_{00} \simeq 1$, one would associate approximate t-channel helicity conservation with those situations depicted in (a) and (c), and approximate s-channel helicity conservation with (b) and (d). Furthermore, (a) shows a strong violation of s-channel helicity conservation, and (b) shows a similar violation of t-channel helicity conservation. However, the configurations depicted in (c) and (d) are quite similar, and only modest changes of dynamics would be needed to pass from one to the other. In these latter situations it is not useful to regard s-channel and t-channel helicity conservation as opposing concepts.

A simple mnemonic is that if approximate helicity conservation is observed, the ideal axis is rotated clockwise (counterclockwise) from the reference axis when the $\mathrm{Re}\rho_{10}$ is positive (negative), i.e., for the configurations shown

$\mathrm{Re}\rho_{10}^t > 0$ in (a), < 0 in (c),

$\mathrm{Re}\rho_{10}^s < 0$ in (b), > 0 in (d).

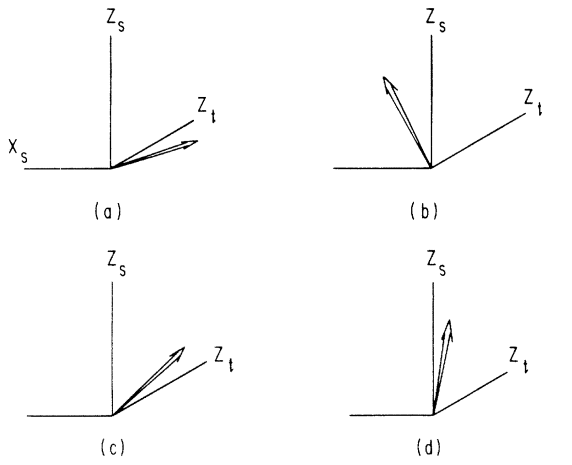

FIG. 3. Illustration of approximate helicity conservation under the hypothesis of exact helicity conservation along the direction denoted by the double arrow. (a) and (c) both display approximate t-channel helicity conservation, while (b) and (d) illustrate approximate s-channel helicity conservation. Experimentally, the processes $\pi p \to (\rho\pi)p$ and $Kp \to (K^*\pi)p$ resemble (c), whereas $Kp \to (\rho K)p$ resembles (b).

The behavior sketched above has been observed and discussed by some experimental groups, notably by the CERN-Serpukhov A_1 collaboration.[5] In their analysis of $\pi p \to (\rho\pi)p$, at 25 and 40 GeV/c, they find a situation similar to that shown in Fig. 3(c), with the ideal axis shifted 10° from the t-channel z axis *toward* the s-channel z axis. Experimentally,[5] $\mathrm{Re}\rho_{10}^t = -0.15 \pm 0.02$. In $Kp \to (K^*\pi)p$, the situation is quite similar. For example, in the combined analysis reported in Ref. 3, $\mathrm{Re}\rho_{10}^t \simeq -0.15$. For $Kp \to (\rho K)p$, however, the experimental situation approximates that shown in Fig. 3(b), with $\mathrm{Re}\rho_{10}^s \simeq -0.10 \pm 0.05$. Thus, the (ρK) system in $Kp \to (\rho K)p$ is close to helicity zero in the s channel and far from helicity zero in the t channel. Data on $Kp \to (\omega K)p$ are less precise, providing a value of $\mathrm{Re}\rho_{10}^s \simeq 0.05 \pm 0.1$, suggesting either diagram (b) or (d) in Fig. 3.

Although our remarks are not strictly valid if nucleon spin-flip occurs, or if the $M = 0$ and 1 amplitudes are not in phase, they nonetheless provide a simple description which allows one to interpret the data easily. In our model calculation, we assume no helicity flip at the nucleon vertex and no phase differences between amplitudes and, therefore, the hypotheses are fulfilled.

III. VECTOR- AND PSEUDOSCALAR-EXCHANGE DECK AMPLITUDES

A. ρ-exchange Deck amplitude for $Kp \to (\rho K)p$

We begin with a detailed analysis of the ρ-exchange graph [Fig. 2(b)] for the specific reaction

$Kp \to (\rho K)p$. The results are generalized easily to vector-exchange graphs for other processes, e.g. ρ exchange in $\pi p \to (\rho\pi)p$, ω exchange in $Kp \to (\omega K)p$, and K^* exchange in $Kp \to (K^*\pi)p$, as we show below.

In Fig. 2(b), the incident K with four-momentum p_2 dissociates into a final K with momentum q_3 and a virtual exchanged ρ of four-momentum $q = (p_2 - q_3)$ and helicity λ_q, $u_2 = q^2$. The lower half of the diagram represents high-energy ρp diffractive elastic scattering. The target has momentum p_1 and helicity λ_{p_1}. The final ρ and the final proton have helicity λ_{q_2} and λ_{q_1}, respectively. The amplitude may be expressed as

$$A_{\lambda_{q_2}\lambda_{q_1},\lambda_{p_1}} = g_{\rho K\bar{K}} \sum_{\lambda_q} \epsilon(\lambda_q)\cdot(p_2+q_3) \times \frac{\exp[b_\rho(u_2 - m_\rho^2)]}{m_\rho^2 - u_2} A^{\mathrm{el}}_{\lambda_{q_2}\lambda_q;\lambda_{q_1}\lambda_{p_1}} . \quad (3.1)$$

In Eq. (3.1), $\epsilon(\lambda_q)$ is the polarization four-vector of the virtual ρ. For the coupling constant, we use the SU(3) relationship $g_{\rho^0 K^+K^-} = 0.5\, g_{\rho^0\pi^+\pi^-}$. The amplitude A^{el} is that for off-shell to on-shell ρp scattering. It is normalized such that $\mathrm{Im}A(t=0) = s_{\rho p}\sigma_{\rho p}$ for on-shell ρp elastic scattering. In addition to the ρ propagator, we include a helicity-independent exponential form factor, whose slope b_ρ is specified below. We use elementary-particle propagators and couplings throughout this paper. Reggeization effects have been found important[13] for a detailed understanding of the shape of the mass spectra and of certain angular distributions. This is certain to be even more true for vector exchange. However, the inclusion of Regge effects here complicates the formalism without leading to any essential modification of our main conclusions.

The mass of the final dissociated $Q(\rho K)$ system is denoted M in Fig. 2(b). Because we are interested in the spin and helicity of the Q, it is useful to examine Eq. (3.1) in either the s-channel rest frame of the Q or in the Gottfried-Jackson t-channel rest frame. The properties of the ρp scattering are most conveniently stated in terms of the s-channel axes, so we choose the s-channel frame of the Q. The final proton momentum defines the z axis. In subsections A 1 and A 2, we discuss the helicity properties of the amplitude A^{el} in Eq. (3.1) and of the $\rho K\bar{K}$ vertex factor $\epsilon(\lambda_q)\cdot(p_2+q_3)$. We then obtain the amplitudes A_0 and A_1 and the cross sections for the production of ρ mesons with s-channel helicity 0 and 1, respectively. These are, of course, only intermediate results since in the end we require helicity amplitudes for Q production. We note, however, that for small t_1 and small M [$\to (m_\rho + m_K)$], the dominant partial wave in the Q system is the S wave. This is true because for small $|t_1|$ a kinematic relationship holds whereby the high partial waves in the ρ propagator are canceled by the diffractive $s_{\rho p}$ factor in Eq. (3.1). This relationship[11] is

$$\frac{s_{\rho p}}{m_\rho^2 - u_2} \simeq \frac{s}{M^2 - m_K^2} . \quad (3.2)$$

In the S wave, the orbital motion makes no contribution to the Q's helicity, and therefore, the ρ helicity controls the Q helicity. At threshold, where $M = (m_\rho + m_K)$, the ρ and Q directions are aligned and the Q and ρ helicities are thus identical. A partial-wave analysis of Eq. (3.1) is presented in subsection C.

1. Virtual-ρ scattering

In order to specify the properties of the virtual to on-shell ρp amplitude A^{el} in Eq. (3.1), we may appeal to data[12] on ρ electroproduction $ep \to e\rho p$, which proceeds according to the vector-dominance diagram in Fig. 2(a). At high energies in the ρp center-of-mass system, the data are consistent with the hypothesis of dominant s-channel helicity conservation at the virtual ρ to on-shell ρ vertex. Specifically, for $-q^2 < 1.4$ GeV^2 and $2.1 < M_{\rho p} < 2.8$ GeV, the helicity single-flip amplitudes are of the order of 15–20% of the nonflip amplitudes for $|t_1| < 0.5$ (GeV/c)^2. Double-flip contributions are even smaller. We therefore ignore all s-channel helicity-flip amplitudes in the ρp scattering. Longitudinal ρ mesons are thus produced by longitudinal virtual ρ's only, and transverse ρ's by transverse virtual ρ's. Data on the ratio $R = \sigma_L/\sigma_T$ of the respective elastic cross sections are reported to be well parametrized as[12]

$$R \equiv \frac{\sigma_L}{\sigma_T} = \xi^2 \frac{(-q^2)}{m_\rho^2} , \quad (3.3)$$

with ξ^2 of the order of 0.5 and independent of $s_{\rho p}$ above 4 GeV^2. The choice $\xi = 1$ corresponds to helicity independence of the cross section for on-shell ρp scattering. This expression may not be valid for $|q^2| \gtrsim 2$ (GeV/c)^2, but we use it only in the region $|q^2| \gtrsim 1$ (GeV/c)^2, where it appears to be satisfactory.

Assuming a purely imaginary amplitude for elastic scattering, and the properties of ρp scattering summarized above, we may write

$$A^{\mathrm{el}}_{0,\lambda_q} = i s_{\rho p}\xi \left(\frac{+q^2}{m_\rho^2}\right)^{1/2} \sigma_{\rho p} \exp\left(\frac{B_\rho t_1}{2}\right) \delta_{0\lambda_q} \quad (3.4)$$

and

$$A^{\mathrm{el}}_{1,\lambda_q} = i s_{\rho p}\sigma_{\rho p} \exp\left(\frac{B_\rho t_1}{2}\right) \delta_{1\lambda_q} . \quad (3.5)$$

We have dropped helicity labels pertaining to the

proton target, λ_{q1} and λ_{p1} in Eq. (3.1). This implies that our amplitude is appropriate only for the dominant case of helicity nonflip at the target-nucleon vertex. Polarization predictions would require consideration in addition of the smaller helicity-flip terms. For the ρp elastic slope B_ρ, and the ρp *total* cross section $\sigma_{\rho p}$, we use values measured in πp scattering, viz., $B_\rho \simeq 8$ (GeV/c)$^{-2}$ and 24 mb, respectively. We note that the amplitudes A_0^{el} and A_1^{el} are specified in the ρp rest frame.

2. *Vertex factor*

The $\rho K\bar{K}$ vertex factor $\epsilon(\lambda_q)\cdot(p_2+q_3)$ in Eq. (3.1) must be evaluated for $\lambda_q = 0, 1$. Because $\epsilon \cdot q = 0$, we may express

$$\epsilon(0) = \frac{\eta}{(|u_2|)^{1/2}}\,(q_z, 0, 0, q_0) \tag{3.6}$$

for longitudinal virtual ρ's, where the virtual-ρ momentum has been written

$$q = (q_0, 0, 0, q_z), \quad q^2 = u_2 . \tag{3.7}$$

In Eq. (3.6), a phase factor η is displayed explicitly, $|\eta|^2 = 1$. We discuss its significance below. For the transverse case,

$$\epsilon(1) = -\frac{1}{\sqrt{2}}(0, 1, i, 0) . \tag{3.8}$$

In a reference frame in which the virtual-ρ momentum and the target-proton momentum are collinear and define the z axis, and in which the vector $(\vec{p}_2 + \vec{q}_3)$ has no y but a positive x component, we find that

$$\epsilon(1)\cdot(p_2+q_3) = \sqrt{2}\,p_{2x} \tag{3.9}$$

and

$$\epsilon(0)\cdot(p_2+q_3) = \eta(|u_2|)^{1/2}\,\frac{(p_{2z}+q_{3z})}{\nu} . \tag{3.10}$$

Here ν is the energy of the virtual ρ in the chosen reference frame. The laboratory frame is a convenient reference frame for reexpressing Eqs. (3.9) and (3.10) in terms of invariants.

3. *Cross sections*

The amplitudes A_0 and A_1 for producing a (ρK) system in which the ρ has s-channel helicity 0 and 1 are obtained by combining Eqs. (3.1), (3.4), (3.5), (3.9), and (3.10). We derive

$$A_1 = ig_{\rho K\bar{K}}\,\frac{\sqrt{2}\,p_{2x}\sigma_{\rho p}}{(m_\rho^2 - u_2)}\,s_{\rho p}\exp\left(\frac{B_\rho t}{2}\right) \times \exp[b_\rho(u_2 - m_\rho^2)]\exp(i\tilde{\Phi}) , \tag{3.11a}$$

$$A_{-1} = -ig_{\rho K\bar{K}}\,\frac{\sqrt{2}\,p_{2x}\sigma_{\rho p}}{(m_\rho^2 - u_2)}\,s_{\rho p}\exp\left(\frac{B_\rho t}{2}\right) \times \exp[b_\rho(u_2 - m_\rho^2)]\exp(-i\tilde{\Phi}) . \tag{3.11b}$$

Here $\tilde{\Phi}$ is the azimuthal angle of the final ρ in the reference frame defined above. It is specified more explicitly in the Appendix. The amplitude for helicity-0 ρ scattering is

$$A_0 = ig_{\rho K\bar{K}}\xi'\,\frac{(-u_2)(p_{2z}+q_{3z})}{\nu(m_\rho^2 - u_2)m_\rho}\,\sigma_{\rho p}s_{\rho p} \times \exp\left(\frac{B_\rho t_1}{2}\right)\exp[b_\rho(u_2 - m_\rho^2)] . \tag{3.12}$$

We note that A_0 is proportional to $(-u_2)$. This factor is obtained from the $(-u_2)^{1/2}$ factors in Eqs. (3.4) and (3.10). It expresses the simple physical requirement that the amplitude for longitudinal vector scattering must vanish when the vector's mass $(-u_2)^{1/2}$ is zero (there are no longitudinal photons). The symbol $\xi' = \xi\eta\sqrt{-1}$. This factor incorporates the possible phase variations which arise when the ρ is moved from the timelike to the spacelike momentum region. In principle it could include a Regge phase for the ρ, as well as phase variation associated with analyticity structure of the overall $(2\to 3)$-body amplitude, and details of the ρp amplitude. Electroproduction data could help in fixing this overall phase, but present results are at too low a value of $s_{\rho p}$ to be useful. Asserting that a diffractive amplitude should have the well-defined phase of $\pm i$ at $t_1 = 0$, we would fix $\xi' = \pm|\xi|$.

With the choices $2g_{\rho K\bar{K}} = g_{\rho^0\pi^+\pi^-}$, $\sigma_{\rho p} = \sigma_{\pi p} = 24$ mb, and $B_\rho = B_\pi = 8$ (GeV/c)$^{-2}$, the only free parameter in Eqs. (3.11) and (3.12) is the ρ form-factor slope b_ρ. Because there is no direct way to extract the value of b_ρ from two-body reaction processes, it remains a free parameter in our calculation. The philosophy we adopt is to select a value of b_ρ which allows us to obtain a consistent description of the helicity properties of the two reactions $\pi p \to (\rho\pi)p$ and $Kp \to (\rho K)p$ in which ρ exchange plays a role. We use the same b_ρ for both reactions and for both amplitudes A_0 and A_1.

Shown in Fig. 4 are the cross sections we obtain by integrating Eqs. (3.11) and (3.12) over three-body phase space. Results are shown for two choices of b_ρ. We display the distribution $d\sigma/dt_1'$ for $Kp \to (\rho K)p$ at 13 GeV/c, for values of $M_{\rho K} \leq 1.35$ GeV. The lab momentum 13 GeV/c is selected to correspond to the energy at which the SLAC data are available.[2] However, our results are essentially independent of incident energy. The restriction $M_{\rho K} \leq 1.35$ is made because the prominent threshold enhancement in the data is confined to this region.[2,3] To be sure, our model

does not provide as sharp an enhancement in the distribution $d\sigma/dM_{\rho K}$ as is seen in the data. We believe that the detailed shape of the mass spectrum is to be understood in terms of the resonance-Deck unitarization procedure of Basdevant and Berger.[14]

A few features of the curves in Fig. 4 should be noted. The cross section $d\sigma_0/dt_1'$ for producing a ρ with s-channel helicity 0 is larger ($\sim \times 4$) than $d\sigma_1/dt_1'$ for all t_1'. This is true for both of the choices made for b_ρ. It will be noted that $d\sigma_1/dt_1'$ does not vanish as $t_1' \to 0$. While it is strictly necessary that the differential production cross section for a (ρK) system with helicity 1 vanish as $t_1' \to 0$, this is not true of $d\sigma_1/dt_1'$. We recall that $d\sigma_1/dt_1'$ is the cross section associated with a ρ of helicity 1. In the (ρK) system, the orbital angular momentum provides a helicity contribution which cancels that of the ρ and thus permits $d\sigma_1/dt_1'$ to remain finite as $t_1' \to 0$. In subsection C we provide a partial-wave analysis of A_0 and A_1.

Before proceeding to a discussion of the partial wave and helicity structure of Eq. (3.1) in the (ρK) rest frame, we remark that the Deck amplitudes lead directly to predictions of the ρ helicity. Subsequent statements regarding the helicity of the ρK system in specific partial waves may be deduced, as we do, but they are less direct tests of the model. The ρ- and K-exchange Deck graphs tend to populate different kinematic regions of the two-dimensional $(\cos\theta, \phi)$ decay angular distribution in the ρK rest frame. A precise isolation of the two contributions is impossible because the mass $M_{\rho K}$ is small and the amplitudes overlap in phase space. Nevertheless, by selecting events in one region of phase space or in another, the contribution of either the ρ- or the K-exchange graph may be enhanced.[9,11] In the purified K-exchange sector, the final ρ should have nearly perfect t-channel helicity 0 (cf. subsection B), whereas in the ρ-exchange sector, the mixture of s-channel helicities derived here should hold.

B. K-exchange Deck amplitude for $Kp \to (\rho K)p$

The form of the pseudoscalar K-exchange Deck amplitude is identical to that of the well-studied π-exchange Deck amplitude.[11] Because pseudoscalar exchange at small t_2 in Fig. 2(c) produces a ρ meson whose t-channel helicity is predominantly zero, we choose to work here with t-channel axes. It may seem inconsistent to use the s-channel axes when discussing the vector-exchange graph and then the t-channel axes for the pseudoscalar-exchange term. In our treatment of the partial-wave structure, we convert the pseudoscalar- (vector-) exchange term to the s-channel (t-channel) basis. However, in dealing here with

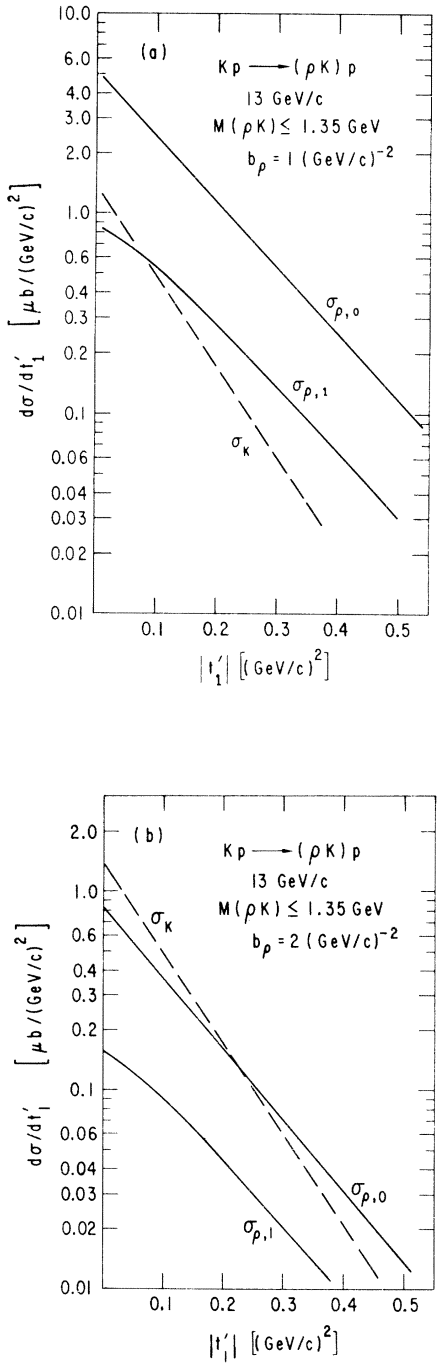

FIG. 4. Distributions $d\sigma/dt_1' dM$ for $Kp \to (\rho K)p$ at 13 GeV/c integrated from threshold to $M_{\rho K} = 1.35$ GeV/c, as obtained from the ρ- and K-exchange Deck amplitudes. In (a) the ρ form-factor slope $b_\rho = 1$ (GeV/c)$^{-2}$ in Eqs. (3.11) and (3.12), whereas in (b) $b_\rho = 2$ (GeV/c)$^{-2}$. The curves are labeled $\sigma_{\rho,0}$ and $\sigma_{\rho,1}$ to denote the cross sections provided by the ρ-exchange amplitudes which lead to final-state ρ's with s-channel helicity 0 and 1. The curve labeled σ_K is the contribution of the K-exchange Deck term.

the full amplitude and the cross sections, it is more convenient to work with the bases which are natural for the two cases, viz., s channel for vector exchange and t channel for pseudoscalar exchange.

The K-exchange Deck amplitude for producing a (ρK) system in which the ρ has t-channel helicity 0 (with the t channel defined in the ρ rest frame) is

$$A_{\lambda_\rho^t=0} = -2g_{\rho K\bar{K}}|\vec{p}_2^{\,\rho}|\frac{\exp[b_K(t_2-m_K^2)]}{m_K^2-t_2} \times is_{Kp}\sigma_{Kp}\exp\left(\frac{B_K t_1}{2}\right). \quad (3.13)$$

Here $|\vec{p}_2^{\,\rho}|$ is the magnitude of the initial K momentum evaluated in the ρ rest frame at $t_2=0$, $|\vec{p}_2^{\,\rho}| = (m_\rho^2 - m_K^2)/(2m_\rho)$. The amplitude defined by Eq. (3.13) generates a (ρK) system having several partial waves and helicities. However, because of the kinematic relationship[11]

$$\frac{s_{Kp}}{-t_2+m_K^2} \simeq \frac{s}{M^2-m_K^2} \quad (3.14)$$

which is valid at small t_1, the predominant partial wave is the S wave. Furthermore, for values of M not too far above the threshold $(m_\rho+m_K)$, the rotation from the boosted t-channel rest frame of the Q to that of the ρ is not large.[7] Thus, Eq. (3.13) provides dominantly an S-wave (ρK) system with t-channel helicity zero.

To obtain a reasonable value for the form-factor slope b_K in Eq. (3.13) and for a consistency check on the magnitude of our K-exchange amplitude, we investigated the two-body process $Kp\to\rho\Lambda$. An experimental analysis[15] at 4.2 GeV/c shows that an unnatural-parity-exchange term is present in $Kp\to\rho\Lambda$ with $\rho_{00}^t \simeq 0.2$, crudely independent of t. An elementary K-exchange contribution to $d\sigma/dt$ for $Kp\to\rho\Lambda$ takes the form

$$\frac{d\sigma}{dt} = \frac{0.3893}{16\pi[s-(m_p+m_K)^2][s-(m_p-m_K)^2]} \times |A_K|^2[(m_\Lambda-m_p)^2-t], \quad (3.15)$$

with

$$A_K = 2g_{\rho K\bar{K}}|\vec{p}^{\,\rho}|\frac{\exp[b_K(t-m_K^2)]}{t-m_K^2}\, g_{\Lambda pK}.$$

The coupling constant $g_{\Lambda pK}^2 = 4\pi(15)$, and $4g_{\rho KK}^2 = g_{\rho^0\pi^+\pi^-}^2 = 4\pi(2.4)$. Here again we evaluate the magnitude of the incident K momentum $|\vec{p}^{\,\rho}|$ in the ρ rest frame at $t=0$. Comparing Eq. (3.15) with the experimental $\rho_{00}d\sigma/dt \simeq 0.2d\sigma/dt$, we find that the choice $b_K = 1$ (GeV/c)$^{-2}$ in Eq. (3.15) provides good agreement with the data in both absolute normalization and t dependence. The same value $b_K \simeq 1$ (GeV/c)$^{-2}$ may be extracted from analyses of the K-exchange component in $Kp\to\rho Y^*$[16]

These comparisons provide some confidence that the form of Eq. (3.13) with the choice $b_K = 1$ (GeV/c)$^{-2}$ will give an accurate estimate of the magnitude of the K-exchange Deck contribution in $Kp\to(\rho K)p$. The cross section $d\sigma/dt_1'$ obtained from Eq. (3.13) is shown (labeled σ_K) as a function of t_1' in Fig. 4 for $M<1.35$ GeV. For the Kp elastic slope B_K and Kp total cross section in Eq. (3.13), we use $B_K = 8$ (GeV/c)$^{-2}$ and $\sigma_{Kp} = 19$ mb. Comparing the magnitudes of the ρ- and K-exchange contributions in Fig. 4, we observe that the ρ contribution is dominant for $b_\rho = 1$ (GeV/c)$^{-2}$, but is comparable to σ_K for $b_\rho = 2$ (GeV/c)$^{-2}$.

C. Partial-wave analysis of $Kp\to(\rho K)p$

The technical details of our method for partial-wave analysis of the Deck amplitudes may be found in the Appendix. We present partial-wave amplitudes $A_M^{JI}(s, M_{\rho K}, t_1)$ for the $l=0$ and $l=1$ states of the ρK system; J is the total spin of the ρK system, and M is its projection along either the s- or the t-channel z axis. The partial waves were computed numerically from expressions in the Appendix. At the values of mass $M_{\rho K}$ considered, the difference between the square of the total amplitude and the sum of the $l=0$ and $l=1$ partial amplitudes is typically 1%. Accordingly we shall not discuss the $l\geq 2$ amplitudes which are in any case sensitive to fine details of our parametrization. The partial waves were initially obtained in the ρK s-channel system of axes for the ρ-exchange Deck terms and in the ρK t-channel system for the K-exchange term. Appropriate rotations about the normal to the ρK production plane were then made to obtain the t-channel amplitudes for ρ exchange, and the s-channel amplitudes for K exchange.

In Fig. 5 we provide the $J^P = 1^+$, $l=0$, and $M=0,1$ partial-wave amplitudes obtained from our ρ-exchange Deck amplitudes. As before, the lab momentum 13 GeV/c corresponds to the energy at which data are available,[2] but our results do not depend on the overall energy of the reaction. The mass selected, $M_{\rho K} = 1.31$ GeV, is in the region of the prominent peak observed experimentally. We choose the form-factor slope $b_\rho = 2$ (GeV/c)$^{-2}$. Our results for the ρ-exchange contribution alone are not sensitive to reasonable variations of b_ρ about this value. However, a small value of b_ρ [~ 1 (GeV/c)$^{-2}$] leads to a ρ-exchange contribution which is unacceptably large in $\pi p\to(\rho\pi)p$, as we discuss in subsection E. Such a small value is also not favored theoretically. It provides a ρ form-factor which barely compensates for the growth of the ρ-exchange Deck amplitudes as a function of $|u_2|$ caused by the momentum factors p_{2x} and $(p_{2z}+q_{3z})$ in Eqs. (3.11) and (3.12). Too large a value of b_ρ

$[>4\ (\mathrm{GeV}/c)^{-2}]$ suppresses the ρ-exchange contribution overly much with respect to K exchange in $Kp \to (\rho K)p$. Thus, the value $b_\rho \simeq 2\ (\mathrm{GeV}/c)^{-2}$ is a reasonable compromise which allows us to obtain approximate s-channel helicity conservation in $Kp \to (\rho K)p$, while preserving approximate t-channel helicity conservation in $\pi p \to (\rho\pi)p$.

In Fig. 5 we show separately the contributions to the $M=0$ and $M=1$ partial waves from the longitudinal $\lambda_\rho = 0$ (top half) and transverse $|\lambda_\rho| = 1$ ρ-exchange Deck amplitudes, Eqs. (3.12) and (3.11),

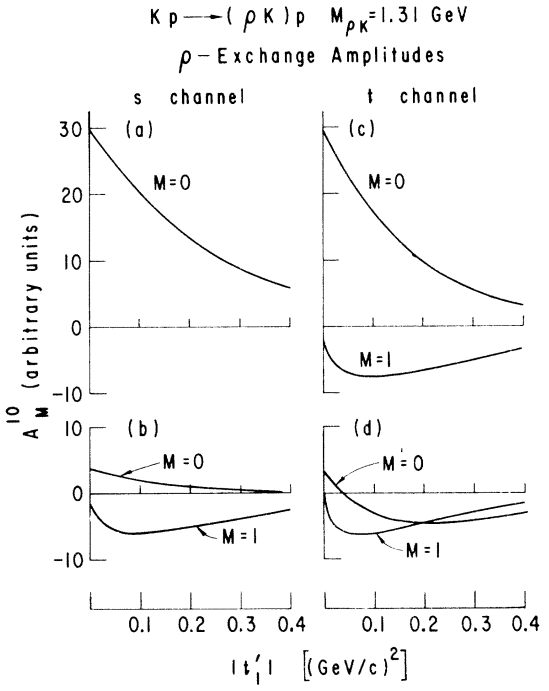

FIG. 5. Amplitudes A_M^{J1} vs $|t_1'|$ for the $J=1$, $l=0$ (S-wave) ρK system in $Kp \to (\rho K)p$ at 13 GeV/c and the mass $M_{\rho K} = 1.31$ GeV obtained from our ρ-exchange Deck amplitudes. In the figure M is the spin projection of the ρK system along a given axis: In (a) and (b), the s-channel axes are used, whereas the t-channel axes are used in (c) and (d). In the top half of the figure, (a) and (c), we display the partial-wave amplitudes obtained from our longitudinal (L) ρ-exchange Deck term (with $\xi' = -1$). In (b) and (d) we present the partial-wave amplitudes from our transverse (T) ρ-exchange Deck amplitude. In (a), the $M=1$ partial wave is negligible on the scale used. For these results $b_\rho = 2\ (\mathrm{GeV}/c)^{-2}$. The net s-channel $M=0$ and $M=+1$ amplitudes provided by our ρ-exchange Deck amplitudes are obtained by combining the contributions shown in (a) and (b); likewise, the net t-channel results by combining (c) and (d). The overall normalization is arbitrary here, but the relative normalization of the curves is fixed by our model. For absolute normalization, consult Fig. 4 or the text.

respectively. It is striking that the $\lambda_\rho = 0$ Deck amplitude has no $M=1$ component in the s channel. There is no similarly simple pattern for the $|\lambda_\rho| = 1$ amplitudes which contribute to both $M=0$ and 1. The common factor of $(-i)$ has been omitted here, so that our partial-wave amplitudes are real for all J, l, M. From parity conservation it follows that $A_M^{Jl} = (-1)^{l+M} A_{-M}^{Jl}$. Therefore, $\rho_{11} = -\rho_{1-1}$ for $l=0$, and $\rho_{11} = +\rho_{1-1}$ for $l=1$.

In Fig. 5, the choice of the sign of the $\lambda_\rho = 0$ ρ-exchange Deck amplitude corresponds to $\xi' = -1$ in Eq. (3.12). With this choice, we find after adding the $\lambda_\rho = 0$ and $|\lambda_\rho| = 1$ contributions that the net s-channel ρ-exchange amplitude A_0^{10} is large and positive, while A_1^{10} is small and negative. Thus, $\mathrm{Re}\rho_{10}^s$ is negative, and the ρ-exchange Deck graph provides the approximate s-channel helicity conservation. However, if we were to reverse the sign of the $\lambda_\rho = 0$ Deck amplitude, setting $\xi' = +1$, the curves in Fig. 5 show that the net would be a near cancellation of the $M=1$ amplitudes in the t-channel, or nearly perfect t-channel helicity conservation for the ρ-exchange Deck contribution. This analysis demonstrates the crucial role played by the sign of the factor ξ' in Eq. (3.12). To obtain the phenomenologically desired result of approximate s-channel helicity conservation for the ρ-exchange Deck graph we cannot set $\xi' = +1$. The choice $\xi' = -1$ leads to approximate s-channel conservation, and it helps to achieve better agreement with the overall normalization of the cross section for $Kp \to (\rho K)p$ and for $\pi p \to (\rho\pi)p$, as described below and in subsection E. The weak point of our presentation is that we are unable to derive the choice $\xi' = -1$ from first principles.

Turning to the K-exchange Deck term, we present its s- and t-channel partial-wave amplitudes A_M^{10} in Figs. 6(a) and 6(c), respectively. From Fig. 6(c), it is apparent that A_1^{10} is very small and negative. The K-exchange Deck amplitude by itself leads to the approximate t-channel helicity conservation situation depicted in Fig. 3(c).

We now consider the results obtained when we combine the ρ- and K-exchange contributions. It would surely be inadmissible to add the Deck amplitudes coherently, since as we have shown, the final ρ emerges from the ρ- and K-exchange Deck graphs with different spin properties. Even at the partial-wave level, different questions of principle may be raised concerning the legitimacy of adding amplitudes obtained from t- (here t_2) and u- (here u_2) channel exchange terms, respectively. On the other hand, neglecting to add the partial-wave amplitudes is also of doubtful validity. In Figs. 6(b) and 6(d), we provide our final s- and t-channel amplitudes A_M^{10} for $Kp \to (\rho K)p$ obtained by adding the K- and ρ-exchange partial waves. With our

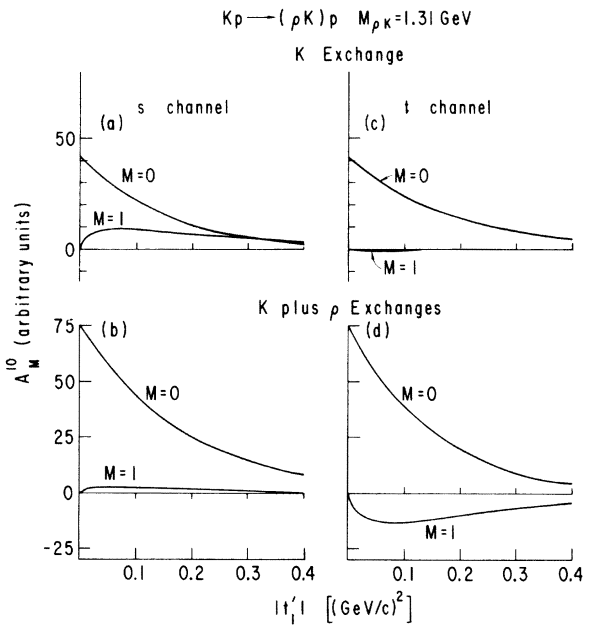

FIG. 6. In (a) and (c), the contribution of the K-exchange Deck term respectively to the s-channel and to the t-channel partial-wave amplitudes A_M^{JI} vs $|t_1'|$ for the $J=1$, $l=0$ (S-wave) ρK system in $Kp \to (\rho K)p$ at 13 GeV/c and $M_{\rho K}=1.31$ GeV. In the figure, M is the spin projection along the s- or the t-channel quantization axis. In (b) and (d) we display the results we obtain after adding the K-exchange and ρ-exchange ($\xi'=-1$) partial-wave amplitudes. The arbitrary scale is the same as used in Fig. 5.

choice of $\xi'=-1$ in Eq. (3.12), we observe that the $\lambda_\rho=0$ ρ-exchange amplitude adds constructively to the K-exchange contribution in the $M=0$ state. The net $M=1$ amplitude is small and positive in the s channel, but it is considerably larger ($\times 7$) and negative in the t channel. Therefore, we obtain nearly perfect s-channel helicity conservation, with $\mathrm{Re}\rho_{10}^s$ very small and positive here. It is evident that a small increase of the ρ-exchange contribution (e.g. by a slight decrease of b_ρ) would move $\mathrm{Re}\rho_{10}^s$ to the negative side of the axis, as data[3] seem to prefer.

For $Kp \to (\rho K)p$, we conclude that with $\xi'=-1$ there is a large range of values of the parameter b_ρ for which the picture of approximate s-channel helicity conservation is maintained in the Deck model. If $\xi'=+1$ were chosen instead, the K- and ρ-exchange amplitudes would tend to cancel each other; for example, at $t_1'=0$ the net $M=0$ amplitude would be ~15 in the units of Figs. 5 and 6, rather than the value ~75 which we obtain with $\xi'=-1$. Stated otherwise, with $\xi'=+1$, the net $\rho+K$ contribution would be a factor of 2 or 3 smaller in the $M=0$ amplitude at $t_1'=0$ than either the ρ or K contribution alone. While such cancellation is possible in principle, we find no physical reason to support its occurrence.[18]

It is instructive to compare the absolute magnitudes of the $J^PM=1^+0$ cross sections we compute with those observed.[2,3] Adding our K- and ρ-exchange amplitudes coherently in the $J^PM=1^+0$ partial wave (with $\xi'=-1$), we obtain the value $d\sigma/dt_1' dM_{\rho K}=0.06$ mb/GeV^3 at $t_1'=0$ and $M_{\rho K}=1.31$ GeV. An experimental result[2] is ~1 mb/GeV^3. Although theoretical estimates are delicate so close to threshold ($\Delta M \sim 50$ MeV here), especially since we work with a ρ of fixed mass and zero width, we believe we have made a careful estimate of the magnitude of the K- and ρ-exchange amplitudes. Accepting the data[2] at face value,[19] we conclude that the order-of-magnitude deficiency of the theory is a real effect in $Kp \to (\rho K)p$. (The disagreement would be even greater for $\xi'=+1$.) This deficiency and the fact that the data show a narrow enhancement near the ρK threshold support a resonance interpretation of the ρK data. In this context, we note that when the Deck model is properly unitarized and one resonance (the Q_B) is coupled to both the $K^*\pi$ and ρK systems,[14] a narrow enhancement is produced in the ρK mass distribution near the threshold. This final-state-interaction effect reinforces the Deck background,[14] potentially by a factor as large as M_Q/Γ_Q in the ρK amplitude. Our present investigation shows that the $J^P=1^+$ ρK system is produced with approximate s-channel helicity conservation, a property we conjecture is maintained in the subsequent coupled-channel rescattering.

The principal s-channel ρK P-wave amplitudes $A_M^{JI=1}$ obtained from our vector-exchange Deck graphs are shown in Fig. 7. For normalization the same scale is used as for the S waves in Figs. 5 and 6. We do not discuss them in detail except to note that they are small.

D. Summary remarks on $Kp \to (\rho K)p$

As described above, the ρ-exchange Deck graphs provide an S-wave $J^P=1^+$ ρK system with s-channel helicity primarily zero, whereas the K-exchange graph yields a system with approximately t-channel helicity zero. Combining the two contributions, we conclude that with $\xi'=-1$ in Eq. (3.12) there is a large range of values of the parameter b_ρ for which approximate s-channel helicity conservation emerges naturally in a Deck model description of $Kp \to (\rho K)p$.

Other features of the data are consistent with our deduction that the ρ-exchange Deck amplitude is important in $Kp \to (\rho K)p$. First, we note that the logarithmic slope of $d\sigma/dt_1'$ is $\simeq 8$ (GeV/c)$^{-2}$

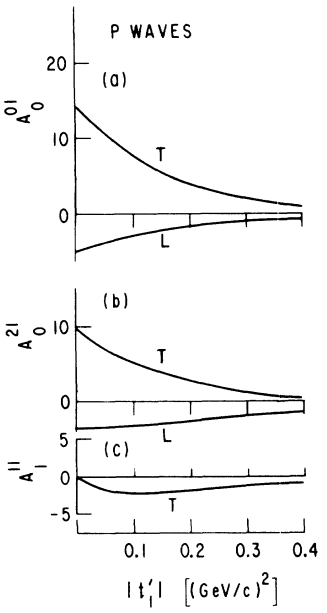

FIG. 7. The s-channel P-wave amplitudes A_M^{JI} for $Kp \to (\rho K)p$ vs $|t_1'|$ at 13 GeV/c and $M_{\rho K} = 1.31$ GeV obtained from our ρ-exchange Deck amplitudes. The contributions of the transverse and longitudinal ($\xi' = -1$) ρ-exchange Deck terms are labeled by T and L, respectively. The $[J, M]$ values are (a) [1, 0] (b) [2, 0], and (c) [1, 1]. In (c), the longitudinal contribution is negligible and is not drawn. Other P-wave amplitudes are smaller than those shown. The scale used is the same as in Figs. 5 and 6.

for the ρ-exchange cross sections $\sigma_{\rho,0}$ in Fig. 4, whereas the slope is $\simeq 10$ (GeV/c)$^{-2}$ for the K-exchange contribution σ_K. The smaller value in the case of ρ exchange arises in the model from the kinematic "feedthrough" to the t_1' variable of the fact that our ρ-exchange amplitude is less peripheral in u_2 than K exchange is in t_2 (cf. Fig. 2). The data[2] show a slope of ~ 8 (GeV/c)$^{-2}$ for the (ρK) system in the same mass region, $M_{\rho K} \simeq 1.3$ GeV, consistent with our expectations.

In our Deck graphs in Fig. 2 only the diffractive (Pomeron-exchange) parts of the ρp and Kp amplitudes are shown. As a result of this simplifying approximation, we obtain identical helicity amplitudes and cross sections for both $K^+p \to (\rho^0 K^+)p$ and $K^-p \to (\rho^0 K^-)p$. Our results are therefore applicable to the average of the data for the two charge states. A description of the differences between the $K^\pm$ reactions would require including the non-Pomeron Regge-exchange terms in the ρp and Kp amplitudes in Figs. 2(b) and 2(c), respectively. One interesting difference has to do with the possible crossover properties[9] of the distributions $d\sigma/dt_1'$ for $K^\pm p \to (\rho^0 K^\pm)p$. Because the ρ is neutral, we note that even with the Regge terms included, the ρp amplitude of Fig. 2(b) will still provide a prediction of identical differential cross sections for the two charge states $K^\pm p \to (\rho K^\pm)p$. The Regge terms in the K-exchange graph provide a crossover of $d\sigma/dt_1'$ which reflects that of elastic scattering, with $d\sigma/dt_1'$ for $K^-p \to (\rho^0 K^-)p$ having a greater slope than that for K^+p. Taking both the ρ and K Deck contributions together, we find that inclusion of the ρ-exchange graph substantially dilutes the crossover, leading to essentially identical differential cross sections $d\sigma/dt_1'$ for $K^\pm p \to (\rho^0 K^\pm)p$, even with all Regge exchanges included. Indeed, the experimenters stressed their observation[2] that the production distributions $d\sigma/dt_1'$ are virtually identical in slope and in normalization for $K^\pm p \to (\rho^0 K^\pm)p$.

Differences between $K^+p \to (\rho^0 K^+)p$ and $K^-p \to (\rho^0 K^-)p$ should be observed if events are selected so as to enhance the contribution of the K-exchange Deck signal. Selections on the s-channel azimuthal angle ϕ_s of the ρ in the (ρK) rest frame have been shown to be effective in separating the contributions from different production mechanisms.[9,11,17] With the definition of the s-channel axes made in Ref. 11, the events with $0 < |\phi_s| < \pi/4$ form a relatively purified sample of data corresponding to the K-exchange Deck graph of Fig. 2(c). In this region, our model predicts $\sigma(K^-) > \sigma(K^+)$, for example, and a crossover of the differential cross sections.

E. Deck amplitudes for $\pi p \to (\rho\pi)p$

The π- and ρ-exchange Deck graphs are shown in Fig. 8. Except for notational changes, the analysis of these amplitudes is identical to that given above for $Kp \to (\rho K)p$. However, we find here that the π-exchange graph provides a much larger cross section than the ρ-exchange term.

The pion-exchange Deck amplitude for producing a $(\rho\pi)$ system in which the ρ has t-channel helicity zero (with the t channel defined in the ρ rest frame) is

$$A_{\lambda_\rho^t=0} = -2g_{\rho^0\pi^+\pi^-}|\vec{p}_2^{\,\rho}|\,\frac{\exp[b_\pi(t_2 - m_\pi^2)]}{m_\pi^2 - t_2} \times i s_{\pi p}\sigma_{\pi p}\exp\left(\frac{B_\pi t_1}{2}\right). \tag{3.16}$$

Here $|\vec{p}_2^{\,\rho}|$ is the magnitude of the initial π momentum evaluated in the ρ rest frame at $t_2 = 0$, $|\vec{p}_2^{\,\rho}| = (m_\rho^2 - m_\pi^2)/(2m_\rho)$. This expression has the same form as that in Eq. (3.13).

The relative magnitudes of the π- and K-exchange Deck amplitudes may be estimated easily. Near $t_1 = 0$, $s_{\pi\rho}/(-t_2 + m_\pi^2) \simeq s/(M^2 - m_\pi^2)$. Thus,

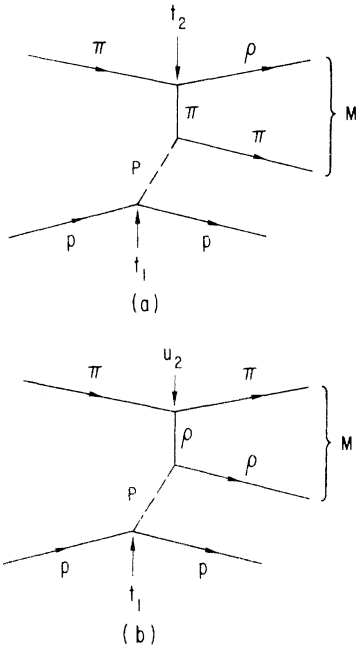

FIG. 8. (a) Pion-exchange Deck diagram for $\pi p \to (\rho\pi)p$. (b) ρ-exchange Deck diagram for $\pi p \to (\rho\pi)p$.

$$\frac{|A(\pi)|}{|A(K)|} \simeq \frac{g_{\rho^0\pi^+\pi^-}}{g_{\rho^0 K\bar{K}}} \frac{(m_\rho^2 - m_\pi^2)}{(m_\rho^2 - m_K^2)} \frac{\sigma_{\pi p}}{\sigma_{Kp}} \times \frac{\exp[b_\pi(t_2 - m_\pi^2)]}{\exp[b_K(t_2 - m_K^2)]} \frac{(M^2 - m_K^2)}{(M^2 - m_\pi^2)} . \quad (3.17)$$

Setting $b_\pi = b_K = 1$ (GeV/c)$^{-2}$, and $M = 1.3$ GeV, we find that

$$\left| \frac{A(\pi)}{A(K)} \right| \simeq 4.6 .$$

The Deck amplitudes for $(\rho\pi)$ production via ρ exchange are identical to those given in subsection A, Eqs. (3.11) and (3.12), but for the replacement of $g_{\rho K\bar{K}}$ by $g_{\rho^0\pi^+\pi^-}$. In Fig. 9 we show the cross sections for $\pi p \to (\rho\pi)p$ predicted by the π- and ρ-exchange Deck graphs. The values $b_\pi = 1$ (GeV/c)$^{-2}$ and $b_\rho = 2$ (GeV/c)$^{-2}$ were used in the π and in the ρ form factors, respectively. Plotted is the t_1' dependence of $d\sigma/dt_1' dM$ integrated from threshold to $M_{\rho\pi} = 1.2$ GeV, the "A_1" region. We observe that the ratio $\sigma_\pi/\sigma_\rho = \sigma_\pi/(\sigma_{\rho,0} + 2\sigma_{\rho,1}) \simeq 24$ at $t_1' = 0$. This demonstrates clear dominance of π exchange over ρ exchange in a Deck-model description of A_1 production at small t_1'. Although ρ-exchange graphs have usually been neglected in previous Deck-model descriptions of $\pi p \to (\rho\pi)p$, ours is the first numerical demonstration that their neglect is justified in this case.

The partial-wave amplitudes A_M^{Jl} for $\pi p \to (\rho\pi)p$

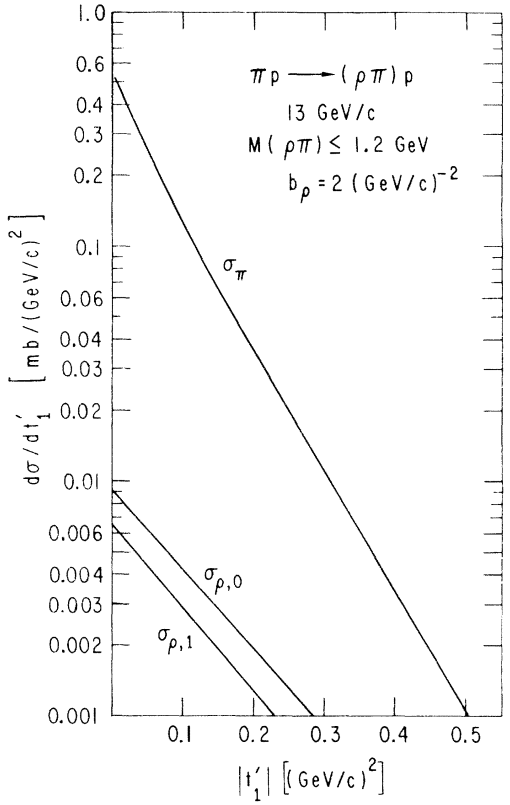

FIG. 9. Distributions $d\sigma/dt_1' dM$ for $\pi p \to (\rho\pi)p$ at 13 GeV/c integrated from threshold to 1.2 GeV as obtained from the Deck model discussed in the text, Sec. II E.

were calculated in exactly the same manner as for $Kp \to (\rho K)p$. In Fig. 10 we present the $J^P M = 1^+0$ and 1^+1 amplitudes obtained from our longitudinal and transverse ρ-exchange Deck terms. The mass $M_{\rho\pi} = 1.07$ GeV is in the region of the "A_1" enhancement. The ρ form-factor slope $b_\rho = 2$ (GeV/c)$^{-2}$. There is little difference between these ρ-exchange amplitudes and those in Fig. 5 for ρK production. Again, the longitudinal ρ-exchange Deck term provides essentially no $M = 1$ contribution in the s channel. Taking $\xi' = -1$ and adding the longitudinal and transverse ρ-exchange contributions, we observe that the ρ-exchange Deck terms in $\pi p \to (\rho\pi)p$ provide a value of $\mathrm{Re}\rho_{10}^s$ which is small and negative, corresponding to the approximate s-channel-helicity-conservation picture sketched in Fig. 3(b).

In the top half of Fig. 11 we present the $J^P = 1^+$ partial-wave amplitudes from our π-exchange Deck term. These amplitudes resemble those in Fig. 6 for K exchange in $Kp \to (\rho K)p$, except that π exchange is much greater in magnitude. The amplitudes show that the π-exchange Deck term provides approximate t-channel helicity conservation,

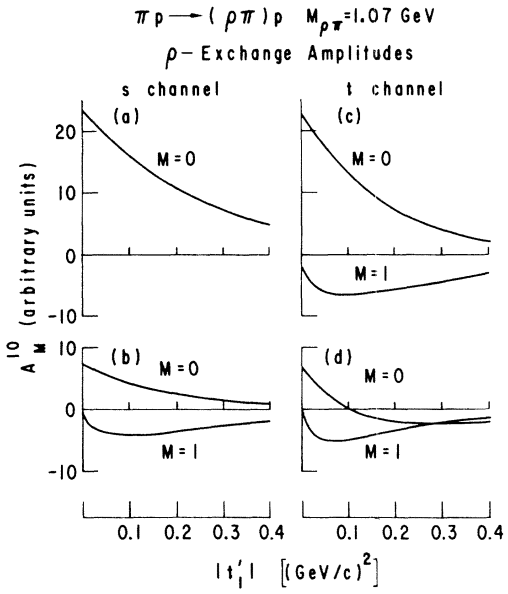

FIG. 10. Amplitudes A_M^{J1} vs $|t_1'|$ for the $J=1$, $l=0$ (S-wave) system in $\pi p \to (\rho\pi)p$ at 13 GeV/c and the mass $M_{\rho\pi}=1.07$ GeV obtained from our Deck amplitudes for the exchange of (a) and (c) longitudinal (L) (with $\xi'=-1$), and (b) and (d) transverse (T) ρ mesons. M is the spin projection of the $\rho\pi$ system along the s-channel axes in (a) and (b), and along the t-channel axes in (c) and (d). In (a) the $M=1$ partial wave is negligible. We use $b_\rho=2$ (GeV/c)$^{-2}$. The overall scale is arbitrary; for normalization consult Fig. 9 and the text.

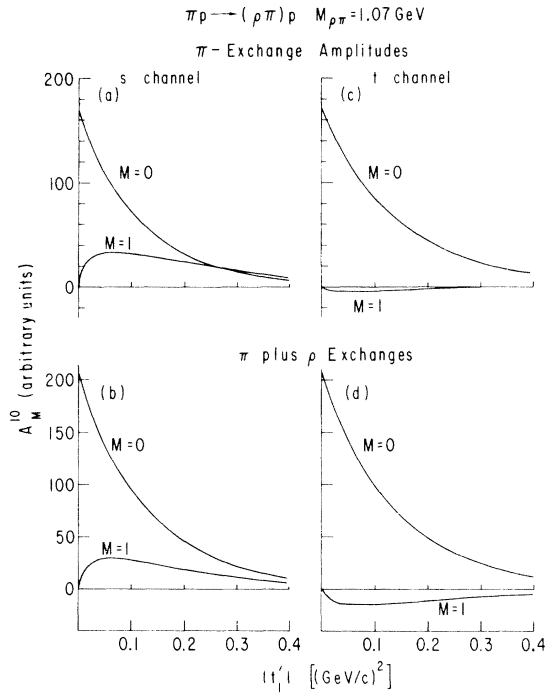

FIG. 11. Contribution of the π-exchange Deck term to (a) the s-channel and (c) the t-channel partial-wave amplitudes A_M^{J1} vs $|t_1'|$ for the $J=1$, $l=0$ (S-wave) $\rho\pi$ system in $\pi p \to (\rho\pi)p$ at 13 GeV/c and $M_{\rho\pi}=1.07$ GeV. In (b) and (d) we display the results we obtain after adding the π-exchange and ρ-exchange ($\xi'=-1$) partial-wave amplitudes. The scale is the same as in Fig. 10.

with $\mathrm{Re}\rho_{10}^t<0$, as depicted in Fig. 3(c).

In the lower half of Fig. 11, we display the net partial-wave amplitudes obtained by summing the π- and ρ-exchange contributions, with $\xi'=-1$ and $b_\rho=2$ (GeV/c)$^{-2}$. In the sum, we observe that $\mathrm{Re}\rho_{10}^s$ is positive and that $\mathrm{Re}\,\rho_{10}^t$ is negative; this is situation (c) of Fig. 3. At $t_1'=-0.08$ (GeV/c)^2, we find that $\mathrm{Re}\rho_{10}^t=-0.12$ and $\mathrm{Re}\rho_{10}^s=0.25$. These results are quite consistent with the data of Ref. 5. At larger $|t_1'|$, our ρ_{00}^t substantially exceeds ρ_{00}^s. Nevertheless, it is clear that t-channel helicity conservation in our model as well as in the data is very approximate. The effect of increasing the parameter b_ρ (decreasing the amount of ρ exchange) is to produce more apparent t-channel helicity conservation. Alternatively, if b_ρ is greatly reduced one passes from situation (c) of Fig. 3 to the approximate s-channel helicity conservation situation (d) of Fig. 3. For example, $b_\rho \leq 1$ is unacceptably small if one wishes to maintain t-channel helicity conservation in $\pi p \to (\rho\pi)p$. The data on the spin systematics of both ρK and $\rho\pi$ production can be described adequately in the Deck model if b_ρ is chosen in the interval (1.5, 2.5).

The overall normalization of the $J^PM=1^+0$ cross section for $\pi p \to (\rho\pi)p$ is reproduced within a factor of 2 by our model. We may compare our results with the data at 40 GeV/c, where the non-Pomeron-exchange contributions have presumably died away. In Ref. 5, the logarithmic slope of the differential cross section and the integrated cross section for production of the $1^+\rho\pi$ S state are quoted as 11.9 ± 1.1 (GeV/c)$^{-2}$ and 72 ± 5 μb, respectively, for $M_{\rho\pi}$ between 1.0 and 1.2 GeV. Converting these figures to an average value for $d\sigma/dt_1'dM_{\rho\pi}$, we find that

$$\frac{d\sigma}{dt_1'dM_{\rho\pi}} \cong 4.3\pm0.3 \text{ mb/GeV}^3$$

at $t_1'=0$ and $M_{\rho\pi}\simeq1.1$ GeV. Our model provides 2.55 mb/GeV^3 for the same quantity. Only 30% of this theoretical value is due to the ρ contribution which we added coherently in obtaining our answer. The logarithmic slope of the theoretical $d\sigma/dt_1'dM$ is 12 (GeV/c)$^{-2}$ in the same mass interval, in excellent agreement with the data. In contrast to the ρK situation, there seems little room for a resonance in the 1^+ S-wave $\rho\pi$ system unless it is very broad.

Owing to the dominance of π exchange, we conclude that in spite of the inclusion of ρ exchange, the traditional Deck prediction of approximate t-channel helicity conservation for the $J^P = 1^+$ state in $\pi p \to (\rho\pi)p$ remains valid.

F. Deck amplitudes for $Kp \to (K^*\pi)p$

The process $Kp \to (K^*\pi)p$ receives contributions from pion exchange and from K^* (vector-) exchange amplitudes. The pion-exchange amplitude is

$$A^{t}_{\lambda_{K^*}=0} = -2g_{K^{*0}K^+\pi^-}|\vec{p}_2^{\,K^*}|\,\frac{\exp[b_\pi(t_2 - m_\pi^2)]}{m_\pi^2 - t_2} \times i s_{\pi\rho}\sigma_{\pi p}\exp\left(\frac{B_\pi t_1}{2}\right). \quad (3.18)$$

It produces a $(K^*\pi)$ system in which the K^* has t-channel helicity zero. Here $|\vec{p}_2^{\,K^*}| = (m_{K^*}^2 - m_K^2)/(2m_{K^*})$ and $g_{K^{*0}K^+\pi^-}{}^2 = 4\pi(1.66)$.

For the K^*-exchange amplitudes, we may follow an analysis identical to that given in subsection A for ρ exchange. Replacing Eqs. (3.12) and (3.11), we derive

$$A^{s}_{\lambda_{K^*}=0} = ig_{K^*K^+\pi^-}\,\frac{F_0\sigma_{K^*p}s_{K^*p}}{(m_{K^*}^2 - u_2)} \times \exp\left(\frac{B_{K^*}t_1}{2}\right)\exp[b_{K^*}(u_2 - m_{K^*}^2)] \quad (3.19)$$

and

$$A^{s}_{\lambda_{K^*}=1} = ig_{K^*K^+\pi^-}\,\frac{\sqrt{2}\,p_{2x}\sigma_{K^*p}}{(m_{K^*}^2 - u_2)}\,s_{K^*p}\exp\left(\frac{B_{K^*}t_1}{2}\right) \times \exp[b_{K^*}(u_2 - m_{K^*}^2)]\exp(i\tilde{\Phi}). \quad (3.20)$$

These are amplitudes for the production of a $K^*\pi$ system in which the final K^* has s-channel helicity 0 and 1, respectively. The factor F_0 in Eq. (3.19) requires a brief discussion. Based on the formalism of subsections A 1 and A 2, F_0 is explicitly

$$F_0 = \frac{\sqrt{u_2}}{m_{K^*}}\,\epsilon(\lambda_{K^*}=0)\cdot(p_2+q_3)\,\xi = \frac{1}{m_{K^*}}\left[\frac{-u_2(p_{2z}+q_{3z})}{\nu} + \frac{|q|}{\nu}(m_K^2 - m_\pi^2)\right]\xi. \quad (3.21)$$

The second term in Eq. (3.21) arises kinematically because the vector K^* couples to unequal mass pseudoscalars. Arguing physically that the amplitude

$$A^{s}_{\lambda_{K^*}=0}$$

should vanish when the exchanged vector's mass is zero, we may elect to drop the second term in Eq. (3.21). The amplitude

$$A^{s}_{\lambda_{K^*}=0}$$

thus becomes linearly proportional to $-u_2$, as is true for the ρ-exchange amplitude in Eq. (3.12). Owing to the unequal-mass kinematics, the point $u_2 = 0$ occurs within the physical region for K^* exchange. Therefore, the amplitude

$$A^{s}_{\lambda_{K^*}=0}$$

contains an additional suppression factor not present for the ρ-exchange amplitudes in $Kp \to (\rho K)p$ and in $\pi p \to (\rho\pi)p$. The result is to reinforce the dominance of the π-exchange amplitude for the description of $Kp \to (K^*\pi)p$. This guarantees that the S-wave $(K^*\pi)$ system is produced primarily with t-channel helicity 0, as is observed experimentally.[2,3]

Explicit numerical results are shown in Fig. 12 for $Kp \to (K^*\pi)p$ at 13 GeV/c, with $M(K^*\pi) \leq 1.35$ GeV and $b_{K^*} = 1$ (GeV/c)$^{-2}$. At $t_1' = 0$ the pion-exchange contribution is a factor of ~10 larger than the sum $\sigma_{K^*,0} + 2\sigma_{K^*,1}$. If the second term in Eq. (3.21) is retained, $\sigma_{K^*,0}$ is increased by a factor of 2.4 at $t_1' = 0$. This leaves the pion-exchange cross section more than a factor of 7 larger than

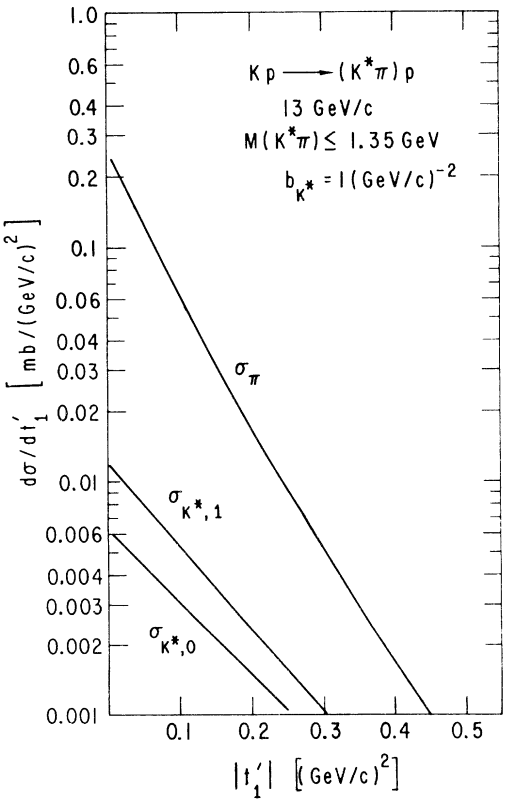

FIG. 12 Distributions $d\sigma/dt_1' dM$ for $Kp \to (K^*\pi)p$ at 13 GeV/c, integrated over the region $M_{K^*\pi} \leq 1.35$ GeV, as obtained from the Deck-model amplitudes discussed in Sec. II F.

the K^* contributions at $t_1' = 0$. Further suppression of the K^* arises if we increase b_{K^*} to 2 $(\mathrm{GeV}/c)^{-2}$. Thus, whichever form is used for F_0, the π-exchange term is dominant and approximate t-channel helicity conservation is expected for the S-wave $K^*\pi$ system.

G. The reaction $Kp \to (\omega K)p$

The analysis of $Kp \to (\omega K)p$ is identical to that given in subsections A–D for $Kp \to (\rho K)p$. In Eqs. (3.11)–(3.13), we need only substitute the symbol ω for ρ everywhere ρ occurs. Because $\sigma_{\omega p} \simeq \sigma_{\rho p}$, $g_{\rho K\bar{K}} \simeq g_{\omega K\bar{K}}$ [according to SU(3)], and $m_\omega \simeq m_\rho$, all numerical results are also identical. Therefore, we conclude as we did for $Kp \to (\rho K)p$, that the Deck model yields approximate s-channel helicity conservation for the $J^P = 1^+$ S-wave ωK threshold enhancement in $Kp \to (\omega K)p$, as is observed in the data.[4] Presence of the ω-exchange graph implies that the production cross sections $d\sigma/dt_1'$ for $K^\pm p \to (\omega K^\pm)p$ should be similar, with no apparent crossover. Because the ρ- and ω-exchange amplitudes are coherent in our description of $Kp \to [(\omega, \rho)K]p$, ρ-ω interference effects should be present in the data.

H. The reaction $Kp \to (\phi K)p$

The amplitudes for $Kp \to (\phi K)p$ need not be presented here. Except for the replacement of p with ϕ, the diagrams are identical to those for $Kp \to (\rho K)p$. Recalling our conclusions for (ρK) and for (ωK) production, we might guess that s-channel helicity conservation will hold also for (ϕK). However, this is not the case. We find that the cross section supplied by the K-exchange Deck graph is more than an order of magnitude greater than that associated with the ϕ-exchange diagrams in the near-threshold region defined by $M_{\phi K} < 1.62$ GeV. This important difference from $Kp \to (\rho K)p$ arises from two factors. First, the amplitude for ϕ production by ϕ exchange includes the factor $\sigma_{\phi p} \simeq 10$ mb, rather than $\sigma_{\rho p} \simeq 24$ mb. Thus, the vector-exchange cross section is reduced by a factor of $(2.4)^2 \simeq 6$ relative to the K-exchange cross section. Second, in the K-exchange amplitude the kinematic factor $(m_\phi{}^2 - m_K{}^2)/2m_\phi$ replaces $(m_\rho{}^2 - m_K{}^2)/2m_\rho$, yielding an increase of a factor of ~ 3 in the K-exchange cross section. These two factors combine to provide dominance of pseudoscalar over vector exchange in the Deck description of $Kp \to (\phi K)p$. Consequently we conclude that the ϕ is produced predominantly with t-channel helicity zero and that the S-wave (ϕK) threshold enhancement should satisfy approximate t-channel helicity conservation. This agrees with available data.[1]

J. The reaction $\pi p \to (K^*\bar{K})p$

In a Deck-model description of $\pi p \to (K^*\bar{K})p$, both K- and K^*-exchange graphs are present. Our numerical results show that the K- and K^*-exchange terms contribute comparable values to the cross section. Neither dominates and thus no simple prediction can be made regarding the helicity of the S-wave threshold enhancement in the $K^*\bar{K}$ system without a more detailed consideration of possible cancellations between the K- and K^*-exchange amplitudes.

IV. CONCLUSIONS

We have investigated the helicity properties of the threshold enhancements in the (1^-0^-) meson systems produced in diffraction dissociation reactions of the type $0^-p \to (1^-0^-)p$. In a Deck-model description of such processes, there are amplitudes for pseudoscalar- (0^-) and vector- (1^-) meson exchange. The pseudoscalar-exchange graphs produce S-wave threshold enhancements with approximate t-channel helicity conservation. The vector-exchange graphs lead to S-wave enhancements which obey approximate s-channel helicity conservation. For a given reaction, the final result depends on the relative weight of the two exchange contributions. For $Kp \to (\rho K)p$ and $Kp \to (\omega K)p$, we determine that the vector- and pseudoscalar-exchange Deck graphs are comparable in magnitude. As a result of a detailed study of the amplitudes we conclude that approximate s-channel helicity conservation holds. However, for $Kp \to (K^*\pi)p$, $\pi p \to (\rho\pi)p$, and $Kp \to (\phi K)p$, the pseudoscalar-exchange Deck graphs dominate the overall cross section, and approximate t-channel helicity conservation is expected. In obtaining these results, we find that two assumptions are required concerning the vector-exchange Deck amplitudes. First, a value must be chosen for the slope b_ρ of the exponential form factor and, second, the overall phase ξ' of A_0 [Eq. (3.12)] is theoretically unknown (to us). All other parameters of both the vector and pseudoscalar amplitudes are fixed *a priori*. Results in agreement with the experimentally observed helicity properties of both $\pi p \to (\rho\pi)p$ and $Kp \to (\rho K)p$ can be obtained if we select $b_\rho \simeq 2$ $(\mathrm{GeV}/c)^{-2}$ and $\xi' = -1$ in Eq. (3.12). These choices provide several other desirable features, including a good representation of both the logarithmic slope and overall normalization[14] of the production differential cross sections $d\sigma/dt_1 dM$ for $\pi p \to (\rho\pi)p$ and for $Kp \to (\rho K)p$. Furthermore, the same considerations, without any new assumptions, lead to a proper description of $Kp \to (K^*\pi)p$, $Kp \to (\omega K)p$, and $Kp \to (\phi K)p$.

In the Q mass region, $M(K\pi\pi) \lesssim 1.4$ GeV, en-

hancements in both the $K^*\pi$ and ρK channels are observed experimentally. Because the $K^*\pi$ system satisfies approximate t-channel helicity conservation whereas the ρK system obeys approximate s-channel helicity conservation, it was suggested that two different dynamical mechanisms are involved, one of which is possibly resonant.[1,3] The different helicity properties have also been emphasized as supportive of the interpretation of the $J^P = 1^+$ $K\pi\pi$ system in terms of two distinct axial-vector resonances.[2,20] In this article we show that the different helicity properties emerge from a single nonresonant dynamical mechanism. The distinction between s- and t-channel helicity conservation is reduced to a matter of whether a pseudoscalar- or a vector-exchange Deck graph is dominant. This numerical question in the model is resolved in terms of known relative coupling strengths. We cannot negate and do not imply to rule out the presence of one or more resonances in the $J^P = 1^+$ $K\pi\pi$ system. Indeed based on structure in the mass spectra and relative phase variations, the case for one resonance, the Q_B, belonging to the $J^{PC} = 1^{+-}$ multiplet seems strong.[14] This resonance couples to both the $K^*\pi$ and ρK channels. Whether a second resonance, the Q_A, is also present in the data is an open question in our view. Our analysis of the helicity structure of the Deck enhancements shows that the Deck "background" on which the resonance (s) is (are) superimposed provides the helicity characteristics seen in the data. The helicity characteristics of the data neither support nor refute the hypothesis that there is resonance activity in the Q region.

APPENDIX: PARTIAL-WAVE ANALYSIS

We suppose that the amplitude for the three-body reaction

$$0^- + \tfrac{1}{2}^+ \to 0^- + j + \tfrac{1}{2}^+$$

$$(p_2 + p_1 \to q_3 + q_2 + q_1)$$

is

$$A_{\lambda_{q_2}\lambda_{q_1}\lambda_{p_1}}(s, t_1, M^2, \theta, \phi)\,,$$

where the spin projection λ_{q_2} refers to some definite choice of axes in the rest frame of the particle of spin j (e.g., s channel, t channel, or other). By a definite choice, we mean that the components of three-vectors are given explicitly. The choice made should be motivated by the dynamics of the model used to calculate the amplitude. The angles θ, ϕ refer to a set of axes in the rest frame of the system $(q_2 + q_3)$, and they define the direction of $\vec{q}_2$ in that frame. Again one may choose any system of axes. Once a definite choice is made, one may define a set of axes in the rest frame of q_2 by a parallel axis transformation. Let $(\tilde{p}, p_0)$ be a four-vector in the $(q_2 + q_3)$ rest frame. Then the boosted momentum is defined by

$$\vec{\tilde{p}}' = \vec{\tilde{p}} + [(\gamma_L - 1)\vec{\tilde{p}} \cdot \hat{e} - \gamma\beta_L p_0]\,\hat{e}\,, \tag{A1}$$

$$p_0' = \gamma(p_0 - \beta_L \vec{\tilde{p}} \cdot \hat{e})\,, \tag{A2}$$

where $\hat{e}$ is a unit vector in the direction (θ, ϕ), and (γ_L, β_L) are the usual Lorentz transformation parameters. If $\vec{p}$ denotes the components of the same four-vector referred to the original choice of axes in the q_2 rest frame, then there exists a rotation (α, β, γ) such that

$$p_\mu = \sum_{\nu=-1}^{1} [D_{\mu\nu}^{1}(\alpha, \beta, \gamma)]^* p_\nu'\,, \tag{A3}$$

where

$$p_{\pm 1} = \mp (p_x \pm i p_y)/\sqrt{2}\,,$$

$$p_0 = p_z\,,$$

and $D_{\mu\nu}^{1}(\alpha, \beta, \gamma)$ is the usual Wigner rotation function. In practice one may solve for (α, β, γ) by selecting the coordinates of some four-vectors in the chosen frames, performing the transformation (A2), and applying (A3). Once the (α, β, γ) are known, the appropriate amplitudes for a partial-wave analysis are obtained as

$$A_{m_s\lambda_{q_1}\lambda_{p_1}}(s, t, M^2, \theta, \phi)$$

$$= \sum_{\lambda=-j}^{j} \left(D^{j}_{\lambda m_s}(\alpha, \beta, \gamma)\right)^* A_{\lambda\lambda_{q_1}\lambda_{p_1}}(s, t, M^2, \theta, \phi)\,. \tag{A4}$$

Here m_s is the spin projection of particle q_2 in the q_2 rest frame along the boosted set of axes. The (α, β, γ) depend on the kinematic variables $(s,\ t,\ M^2, \theta,$ and $\phi)$.

Given these amplitudes, the partial-wave analysis proceeds by analogy with the nonrelativistic addition formula[21]

$$A_{m_s\lambda_{q_1}\lambda_{p_1}}(s, t, M^2, \theta, \phi)$$

$$= \sum_{J, l, M} A^{J, l}_{M\lambda_{q_1}\lambda_{p_1}}(s, t, M^2) \sum_{m_l=-l}^{l} C^{ljJ}_{m_l m_s M}\, Y_l^{m_l}(\theta, \phi)\,. \tag{A5}$$

The

$$A^{J, l}_{M\lambda_{q_1}\lambda_{p_1}}(s, t_1, M^2)$$

are the partial-wave amplitudes, $C^{ljJ}_{m_l m_s M}$ is a Clebsch-Gordan coefficient, and $Y_l^{m_l}(\theta, \phi)$ is a spherical harmonic. The

$$A^{J, l}_{M\lambda_{q_1}\lambda_{p_1}}$$

may then be obtained by integration,

$$A^{JI}_{M\lambda_{q_1}\lambda_{p_1}}(s,t_1,M^2) = \int d\cos\theta\, d\phi \sum_{m_l m_s} C^{ljJ}_{m_l m_s M} Y^{m_l *}_{l}(\theta,\phi) \times A_{m_s\lambda_{q_1}\lambda_{p_1}}(s,t,M^2,\theta,\phi), \tag{A6}$$

The normalization is such that

$$\int d\cos\theta\, d\phi \left(\sum_{\lambda=-j}^{j} A_\lambda A_\lambda^*\right) = \sum_{J,l,M} |A^{JI}_M|^2 .$$

We have dropped nucleon spin indices in this last equation.

The results reported in the text were obtained by standard numerical integration. The various axes used were as follows.

In the Q rest frame we used

t channel: $\vec{p}_2$ along positive z direction; $[\vec{p}_2 \times (-\vec{q}_1)]$ along positive y direction.

s channel: $\vec{q}_1$ along negative z direction; $(\vec{p}_1 \times \vec{q}_1)$ along positive y direction.

In the ρ (or particle q_2) rest frame we used

t-channel axes: $\vec{p}_2$ along positive z direction; $\vec{p}_2 \times [-(\vec{q}_1 + \vec{q}_3)]$ along positive y direction.

s-channel for "ρ"$p \to \rho p$: $\vec{q}_1$ along negative z direction; $(\vec{p}_1 \times \vec{q}_1)$ along positive y direction.

The correct threshold properties of the A^{JI}_M, namely

$$A^{JI}_M \propto |t_{1\min} - t_1|^{|M|/2} \text{ as } t_1 \to t_{1\min}$$

and

$$A^{JI}_M \propto [M - (m_{q_2} + m_{q_3})]^{I/2} \text{ as } M \to (m_{q_2} + m_{q_3}),$$

provide useful checks on the numerical analysis. We remark that in the ρ rest frame the direction of the t-channel y axis may vary rapidly as a function of the kinematic variables; proper care is thus necessary in the numerical integration.

The azimuthal angle $\tilde{\Phi}$ appearing in Eq. (3.11) is the standard Φ angle in a Jacob-Wick expansion of the virtual ρp elastic scattering amplitude. It may be defined as follows: In the center-of-momentum frame for the virtual ρ-proton collision, let the virtual-ρ momentum be along the positive z direction, and let p_2 have a positive x component, with no y component. Then $\tilde{\Phi}$ is the azimuthal angle of the final ρ, as seen in this system. This angle may be expressed in terms of other angles or invariants. A useful quantity for obtaining explicit expressions is

$$\epsilon_{\mu\nu\lambda\sigma} p_1 p_2 q_2 q_3 ,$$

which is proportional to $\sin\Phi$.

---

*Work performed under the auspices of the United States Energy Research and Development Administration.

†Permanent address.

‡Équipe de Recherche Associée au C. N. R. S.

[1]For a summary of experimental results and a comparison of various processes, a consult P. Bosetti *et al.*, Nucl. Phys. B101, 304 (1976).

[2]G. W. Brandenburg *et al.*, Phys. Rev. Lett. 36, 706 (1976).

[3]G. Otter *et al.*, Nucl. Phys. B106, 77 (1976).

[4]Aachen-Berlin-CERN-London-Vienna and Birmingham-Brussels-CERN-Mons-Serpukhov Collaborations, CERN Report No. CERN/EP/Phys. 76, 1976, submitted to the Tbilsi Conference (unpublished).

[5]Yu. M. Antipov *et al.*, Nucl. Phys. B63, 153 (1973).

[6]S. Drell and K. Hiida Phys. Rev. Lett. 7, 199 (1961); R. Deck *ibid.* 13, 169 (1964); E. L. Berger, Phys. Rev. 166, 1525 (1968); 179, 1567 (1969).

[7]J. T. Donohue, Nucl. Phys. B35, 213 (1971); C. D. Froggatt and G. Ranft, Phys. Rev. Lett. 23, 943 (1969).

[8]G. W. Brandenburg *et al.*, Nucl. Phys. B45, 397 (1972).

[9]E. L. Berger Phys. Rev. D 11, 3214 (1975).

[10]I. Butterworth (private communication).

[11]E. L. Berger, in *Proceedings of the Daresbury Meeting on Three Particle Phase Shift Analysis and Meson Resonance Production,* edited by J. Dainton and A. J. G. Hey (Daresbury Laboratory, Daresbury, 1975). A summary of useful kinematic relationships may be found in the Appendix of this reference.

[12]DESY-Glasgow-Hamburg Collaboration, P. Joos *et al.*, report, 1976 (unpublished). A useful description of virtual-photon–nucleon elastic scattering is found in K. Schilling and G. Wolf, Nucl. Phys. B61, 381 (1973).

[13]E. L. Berger, Ref. 6.

[14]J. L. Basdevant and E. L. Berger, Phys. Rev. Lett. 37, 977 (1976).

[15]A. J. deGroot *et al.*, Nucl. Phys. B74, 77 (1974).

[16]R. Worden, analysis based on 4.2-GeV/c Amsterdam-CERN-Nijmegen-Oxford data, as quoted by F. Schrempp and B. Schrempp, in *High Energy Physics,* proceedings of the European Physical Society International Conference, Palermo, 1975, edited by A. Zichichi (Editrice Compositori, Bologna, 1976); cf. Fig. 13 and Eq. (20).

[17]P. Bosetti *et al.*, Nucl. Phys. B103, 189 (1976).

[18]Although $\xi' = +1$ is clearly not acceptable from a phenomenological point of view, we remark that the choice $\xi' = \pm i$ yields essentially identical results for the density matrix as our favored choice $\xi' = -1$, and is thus also acceptable phenomenologically. However, the choice $\xi' = \pm i$ would mean that the amplitude A_0 in Eq. (3.12) is purely real, unusual for a diffractive production

amplitude. The principal difference between the numerical results is that the $Kp \to (\rho K)p$ cross section for $\xi' = \pm i$ is about 0.5 that for $\xi' = -1$. Similar behavior holds in $\pi p \to (\rho\pi)p$, discussed in Sec. II E. In this latter reaction, $\xi' = \pm i$ leads to slightly better approximate t-channel helicity conservation, with a reduction in cross section by a factor of $\sim\frac{2}{3}$. The presence of a phase factor such as $\xi' = \pm i$ would be indicated experimentally by a violation of the equality

$$(\mathrm{Re}\rho_{10})^2 = 0.5\rho_{00}(1-\rho_{00}),$$

which holds exactly in our equal-phase spinless-nucleon model.

[19]We are concerned of course that K-π ambiguity problems, for example, could lead to an experimental overestimate of the size of the ρK cross section. In Yu. M. Antipov *et al.*, Nucl. Phys. B86, 381 (1975), it is concluded that the "data are consistent with zero genuine $1^+(S \to \rho K)$ events, and that the fraction of $1^+(S \to \rho K)$ events obtained from the partial-wave analysis can be explained by ambiguous events..." belonging to $1^+(S \to K^*\pi)$. Furthermore, these experimenters quote a cross section of $26 \pm 3\ \mu$b at 40 GeV/c for the $1^+(S \to K^*\pi)$ wave in the mass interval 1.2 to 1.4 GeV and the momentum transfer interval 0.05 to 0.6 $(\mathrm{GeV}/c)^2$, as well as a $K\rho/K^*\pi$ intensity ratio of 0.05 ± 0.10 in the 1^+ state. Adopting an average production slope of 10 $(\mathrm{GeV}/c)^{-2}$, we derive $d\sigma/dt'dM = (2.15 \pm 0.25)$ mb/GeV^3 from these data at $t' = 0$ and $M_{K^*\pi} \simeq 1.3$ GeV. Thus for ρK, these data would suggest a value of $d\sigma/dt'dM_{\rho K} \simeq 0.1 \pm 0.2$ mb/GeV^3 at $t' = 0$ and $M_{\rho K} = 1.3$ GeV. The central value of this latter estimate is only a factor of 2 greater than our theoretical estimate.

[20]M. G. Bowler, Oxford Report No. Ref. 48/76, 1976 (unpublished).

[21]G. Ascoli, L. Jones, B. Weinstein, and H. W. Wyld, Jr., Phys. Rev. D 8, 3898 (1973).